# Interplot Interference: A Model for Planning Field Experiments with Aerially Disseminated Pathogens

R. E. Paysour and W. E. Fry

Department of Plant Pathology, Cornell University, Ithaca, NY 14853. Present address of senior author: Business School, Cornell University.
This work was supported in part by USDA Grant 58-32U4-0-168.
Accepted for publication 16 January 1983.

## ABSTRACT

Paysour, R. E., and Fry, W. E. 1983. Interplot interference: A model for planning field experiments with aerially disseminated pathogens. Phytopathology 73:1014-1020.

A model of disease gradients was used to compute the relative quantities of aerially dispersed, infective inoculum lost from and exchanged between experimental field plots. These quantities were included in a model of disease development to estimate the influence of negative and positive interplot interference on research results. The magnitude of inoculum loss and exchange was a function of plot size, shape, spacing between plots, and steepness of the disease gradient. Neighboring plots that differed markedly in disease severity were more influenced by interplot interference than were plots with similar disease severities. Plot sizes and spacings that limited interplot interference to acceptable levels were identified. The models were quantified and some predictions were validated for potato late blight in New York.

The interpretation of experimental results from small field plots is often hampered by the failure of those plots to accurately represent large commercial fields. A major cause of this problem is "interplot interference," which can be especially important in experiments with aerially disseminated pathogens (7–9). James and co-workers (7) described two types of interplot effects, which they termed negative and positive interference. Negative interference occurs when a large proportion of the inoculum produced within a plot is dispersed outside that plot's boundaries. Epidemic development is limited since the lost inoculum cannot contribute to further infections. Conversely, positive interference occurs when a plot is subjected to an influx of inoculum from external sources (ie, other plots in the experiment), resulting in enhanced epidemic development. All experimental plots are subject to both negative and positive interference; however, all plots are not affected equally. An important consequence is that differences between treatments are sometimes significantly smaller in experimental plots than they would be in large fields. Economic aspects, such as the level of required disease control, can be greatly misinterpreted if based upon data affected by high levels of interplot interference.

Vanderplank (14) pointed out the importance of interplot interference (or "cryptic error") and considered several elements that play a role in determining its magnitude. Despite this attention, a precise means of dealing with the problem does not yet exist. Some practices (eg, planting guard rows and leaving alley ways) are commonly used to reduce interplot interference; however, there are no quantitative guidelines.

The purpose of this study was to construct a general mathematical model of interplot interference that could be used to develop recommendations for limiting the effects of such interference. In this paper, we quantitatively describe how interplot interference is influenced by plot size, shape, treatment differences, spacing between plots, and dispersal characteristics of various pathogens. We then show how this information can be used to plan field experiments in which interplot interference would be limited to acceptable levels. Some predictions of the model are validated for potato late blight on an experimental farm in New York. Some of these results have appeared in a preliminary report (12).

The publication costs of this article were defrayed in part by page charge payment. This article must therefore be hereby marked "*advertisement*" in accordance with 18 U.S.C. § 1734 solely to indicate this fact.

## MATERIALS AND METHODS

**Model.** Our model of interplot interference consists of two components. The first component describes the movement of infective inoculum within a field ("infective inoculum" is defined here as inoculum that would cause infection if it were deposited within the confines of a healthy crop canopy). Inoculum can move both out of an experimental plot (inoculum loss, which causes negative interference) and into it (inoculum gain, which causes positive interference). The impact of this inoculum movement on epidemic progression in each plot is then assessed by using the second component of our model, which describes disease development in time.

**Inoculum movement.** The description of the movement of infective inoculum is based on observations of primary disease gradients that result from point inoculum sources. When the level of disease is low and multiple infections are insignificant, primary disease gradients can be used to infer the movement of infective inoculum. Several models of disease gradients are presented in the literature (6,10,11,15). We selected one proposed by Kiyosawa and Shiyomi (10) because its parameters are readily estimated and its mathematical form is convenient. In this model, disease intensity after one cycle of spore dispersal declines exponentially with distance from a point source of inoculum (equation 1).

$$z = ae^{-bx} \tag{1}$$

in which $z$ = the number of infections per unit area at the target site, $x$ = the distance from the point source to the target site, $a$ = the number of infections per unit area at the source (this is a scaling factor that reflects the strength of the inoculum source), and $b$ = a factor describing disease gradient steepness.

The disease gradient results from a deposition gradient of infective spores. Thus, at low disease levels, "$b$" indicates the pathogen's dispersal pattern of infective inoculum. Pathogens whose infective spores are deposited mostly near the source produce steep disease gradients characterized by a large "$b$". The value of this parameter becomes smaller for gradients caused by pathogens whose infective spores are dispersed relatively greater distances.

The disease gradient model is modified to describe movement of infective spores in an experimental field by expanding it to two dimensions and by including multiple point sources of inoculum. Two dimensions are easily incorporated in the model by modifying equation 1 to

$$z = ae^{-b\sqrt{[(q-q_i)^2 + (p-p_i)^2]}} \tag{2}$$

which gives the infections per unit area, $z$, as a function of distance from the point source $(q_i, p_i)$ to the target $(q,p)$ along both the $q$ and $p$ axes of a Cartesian plane. Multiple point sources are included by summing the gradients caused by each inoculum source in a source plot. This is represented as

$$z = \sum_{i=1}^{n} ae^{-b\sqrt{[(q-q_i)^2 + (p-p_i)^2]}} \tag{3}$$

in which $n$ is the number of individual inoculum sources within the plot.

Equation 3 is used to calculate the relative number of infective spores produced within a plot that fall within or beyond that same plot's boundaries. It is also used to calculate the relative number of infective spores produced within a plot that are deposited in any other plot. This is done by integrating over $q$ and $p$ and selecting the proper region of integration. It is represented by

$$S = \sum_{i=1}^{n} \int_{l_1}^{u_1} \int_{l_2}^{u_2} a \cdot e^{-b\sqrt{[(p-p_i)^2 + (q-q_i)^2]}} \, dq\,dp \tag{4}$$

in which $S$ = number infective spores produced by the plot that are deposited in plot or target area $Q$, $l_1, u_1$ = boundaries of plot $Q$ on $q$ axis, and $l_2, u_2$ = boundaries of plot $Q$ on $p$ axis. The solution of $S$ was numerically approximated on a computer.

The total number of infective spores, $S_\Sigma$, produced in a given plot is found by integrating over $q$ and $p$ from $-\infty$ to $+\infty$. This integral was solved analytically (equation 5).

$$S_\Sigma = n \cdot 2 \cdot \pi \cdot a / b^2 \tag{5}$$

The proportion of infective spores ($v$) produced in a plot that land within a target area $Q$ is then

$$v = S / S_\Sigma \tag{6}$$

This target area can either be the source plot (indicating the proportion of infective inoculum retained by a plot) or any other plot of the experiment (indicating the proportion of infective inoculum exchanged between plots).

**Impact of inoculum movement on epidemic development.** The effect of inoculum loss and exchange on epidemic progression in small plots was estimated by using a submodel that described disease development in time. Inoculum loss from a plot was assumed to reduce pathogen infection efficiency, which for our purposes is defined as the proportion of spores produced by a pathogen that would cause lesions if availability of healthy tissue was not limiting. For simplicity, we assumed the proportion of inoculum loss calculated by equation 6 to be constant throughout the season.

To demonstrate the generality of our methods, two widely differing submodels were used to describe disease development in time. The first submodel was a simplified version of Bruhn's (2) potato late blight simulator, which accurately characterizes epidemics in our experimental system. The impact of inoculum loss was evaluated by altering the parameter that describes pathogen infection efficiency.

The second submodel was a discrete version of the logistic equation of population growth (equation 7) (13). The term $(1 - Y_t)$ is needed, because late in the epidemic multiple infections prevent some infective inoculum (as we define it) from causing new lesions.

$$Y_{t+1} = Y_t e^{r_t (1 - Y_t)} \tag{7}$$

in which $Y_t$ = proportion disease at time $t$, and $r_t$ = pathogen's intrinsic rate of increase at time $t$. The parameter $r_t$ can be approximated from equation 8 (13).

$$r_t = (1n\ m_t) / T \tag{8}$$

in which $m_t$ = the number of new lesions that would be produced in the next generation for each lesion present in the plot at time $t$, if availability of healthy tissue was not limiting and $T$ = the mean generation time of the pathogen. The loss of inoculum from a plot results in a lower value of $m_t$ and hence, slower epidemic growth rate.

Equation 7 can also be employed to assess the impact of inoculum gain. The amount of inoculum gained by a plot is affected by the difference in disease severity between that plot and neighboring plots. Since these differences change throughout a season, the level of inoculum gain must change also. We incorporated this change by recomputing $r_t$ for each day of the season. The variable $m_t$ is calculated as

$$m_t = F\left[NS_\Sigma(o,t) + \sum_{i=1}^{w} P_i S_\Sigma(i,t)\right] / Y_t K \tag{9}$$

in which $F$ = the infection efficiency of pathogen when negative interference is zero, $N$ = the proportion of infective inoculum retained by the plot, $S_\Sigma(o,t)$ = total inoculum produced during the next generation by all lesions present in plot on day $t$, $P_i$ = the proportion of infective inoculum produced by neighboring plot $i$

that is deposited in the plot, $w$ = the number of neighboring plots, $S_\Sigma(i,t)$ = total inoculum produced during the next generation by all lesions present in neighboring plot $i$ on day $t$, and $K$ = the maximum number of lesions that can occur in the plot. The variable $r_t$ is then computed from equation 8. A simple algorithm was written to solve equations 7–9 on a computer and thus simulate epidemic development in each plot of an experimental field.

**Parameter estimation.** The two parameters of equation 3, $a$ and $b$, were estimated for our experiments with potato late blight by examining primary disease gradients in both sprinkler-irrigated and nonirrigated potatoes (*Solanum tuberosum* L.). The irrigated potatoes were planted on 27 May 1981, with foundation seed (whole tubers) of cultivar Katahdin at a spacing of about 0.9 m between and 0.45 m within rows. Plots consisted of four rows, each about 4 m long, and at least 4.5 m of fallow ground surrounded all plots. Published disease gradients for potato late blight (15) caused us to believe that these spacings would produce negligible inoculum exchange among plots. Fertilizer (133.5 kg N, P, and K per hectare) and insecticide (aldicarb 15 G, 2.67 kg [a.i.]/ha) were applied at planting, and an herbicide (linuron 50 WP, 2.67 kg [a.i.]/ha) was applied just prior to emergence. Additional insecticide (parathion 8 F, 0.45 kg [a.i.]/ha) was applied during the season as needed.

Two plots were inoculated at 2100 hours, 26 July 1981. The five most terminal leaflets of six fully expanded leaves, located in the approximate plot center 10–60 cm above ground, were inoculated. A 10-$\mu$l droplet of a sporangial suspension (400 sporangia per microliter) was placed on the abaxial surface of each leaflet. For 24 hr following inoculation, the entire stem was covered with a plastic bag to prevent spore splashing. Inoculum was obtained from 10- to 14-day-old cultures of *Phytophthora infestans* race (1,3,4) grown at about 18 C on amended lima bean agar (1).

Over the next 2 wk, conditions conducive to the development of potato late blight were maintained by sprinkler irrigating the plots from 0730 to 0800 hours each morning (1.56 mm water per hour). Under these conditions, the incubation and latent periods of the fungus were at least 3 and 5 days, respectively. Disease spread was assessed 12 days after inoculation so that all lesions present were initiated by first-generation progeny of initial infections. The primary gradient was quantified by dividing the plots into a $7 \times 7$ matrix of $0.5 \times 0.5$-m cells. Since the disease gradient would be used to deduce the deposition of infective inoculum, foliage that had significant levels of multiple infections could not be sampled. As a result, in irrigated plots only foliage higher than 20 cm above ground level was examined because the lower part of the canopy was heavily infected. Five stems from each cell were randomly selected and potato late blight lesions were counted on all fully expanded leaves (about 5–10 per stem). The parameters $a$ and $b$ were estimated by regressing the natural logarithm of the average number of lesions per leaf against distance from the inoculum source.

The procedures used to estimate $a$ and $b$ in nonirrigated potatoes were similar to those described above, except plots were larger (four rows about 9 m long) and the cultivar Kennebec was planted. No supplemental irrigation was applied and, in some cases where multiple infections were not significant, leaves from the lower part of the canopy were included in the sampling.

**Model validation.** The models were used to predict a relationship between plot size and epidemic severity. Model validation was initiated by comparing this prediction with actual potato late blight development in field plots of various sizes. Experiments were conducted during two seasons. In 1980, square plots of four different areas (0.81, 7.29, 20.25, and 39.60 $m^2$) were established in a randomized-complete-block design. The three smallest plot sizes were replicated three times each for two potato cultivars, Sebago and Hudson. The largest plot size was replicated only twice for each cultivar. A 0.9-m-wide border of potatoes was planted around each plot to minimize microclimatic differences between small and large plots due to edge effects. Borders were not expected to contribute to epidemic development since the cultivar planted, Kennebec, is highly resistant to the race of *P. infestans* used in this study. Plots were hand planted 28 May with certified seed spaced 0.9-m between, and 0.23-m within, rows. At least 4 m of fallow and border separated the experimental units. Insecticide and herbicide applications were similar to those described previously.

Epidemics were initiated 2000–2100 hours on 21 July by spraying plots with a water suspension of *P. infestans* race 0 containing ~50 sporangia per milliliter. The inoculum was uniformly distributed over each plot at a rate of about 33 ml/$m^2$ of plot area. Inoculations were repeated the following three nights to ensure disease establishment. Plots were sprinkler irrigated from 0730 to 0800 hours and 1900 to 1930 hours each day during the next 5 wk to maintain conditions favorable for disease development. Epidemic development was measured by visually assessing plots every 2–5 days on the basis of a previously described key (4). The area under the disease progress curve was calculated as previously described (5) in order to compare epidemics.

In 1981, a second experiment was conducted in five sizes of square plots (0.81, 3.24, 7.29, 12.96, and 29.16 $m^2$) planted to cultivar Katahdin. A completely randomized design was used with four replications of each treatment. Cultural conditions were similar to those in the 1980 plot size experiment. Epidemics were initiated 2100–2300 hours on 23 July, by applying 10 $\mu$l droplets of inoculum (*P. infestans* race 0 containing 225,000 sporangia per milliliter) to the adaxial surface of the five most terminal leaflets of selected leaves. Inoculated leaves were uniformly distributed throughout the plot with one leaf chosen per 0.81 $m^2$ of plot area. Four days after epidemic initiation, inoculated leaves were trimmed so that only one visible lesion per leaf remained. This established an initial disease level (proportion infected tissue) that was equal and precisely quantified for all plots. Epidemic development was measured as described previously and AUDPC and the apparent infection rate were calculated for each plot. Apparent infection rates were calculated by regressing the logit of proportion tissue affected against time for the interval between 5 and 21 days after epidemic initiation. During this period, the proportion of tissue affected increased from an initial level of 0.0001 to about 0.35 in the most heavily infected plots.

TABLE 1. Predicted effect of plot shape on proportion of inoculum lost from rectangular 25 $m^2$ plots[a]

| Plot dimensions (m × m) | Proportion of inoculum lost |
|---|---|
| 0.5 × 50.0 | 0.8474 |
| 1.0 × 25.0 | 0.7245 |
| 2.0 × 12.5 | 0.5600 |
| 3.0 × 8.33 | 0.4742 |
| 4.0 × 6.25 | 0.4366 |
| 5.0 × 5.0 | 0.4271 |

[a] Calculated from Equations 4–6 with parameter values of $b = 1.0\ m^{-1}$, $a = 10$. The value of $a$ is actually irrelevant since this parameter cancels out.

## RESULTS

**Factors affecting level of inoculum loss.** The influence of plot size, shape, and steepness of the disease gradient on the proportion of infective inoculum lost from plots was predicted using equations 4–6 (all inoculum referred to hereafter is restricted to that which is infective). Inoculum loss is lowest in square plots and increases as plots become narrower and longer (Table 1). This relationship is modified quantitatively by different plot sizes or values of $b$; however, the general form remains the same, ie, inoculum loss is minimized in square plots. Subsequent analyses with the models are done with square plots only.

The proportion of inoculum lost from plots decreases with increasing plot size (Fig. 1) and approaches an asymptotic limit of zero in very large plots. The exact form of this relationship is strongly influenced by the steepness of the disease gradient ($b$). For plots of fixed size, inoculum loss is higher when the disease gradient is flatter. The following example illustrates this point. We used data from the literature to estimate steepness of disease gradients produced by *Puccinia polysora* in corn (3) and *P. infestans* in potatoes (15). The values of $b$ were ~0.25 $m^{-1}$ and ~1.0 $m^{-1}$ for corn rust and late blight, respectively. Using these estimates, Fig. 1

indicates that about 43% of the inoculum produced is lost from 25 $m^2$ square potato plots uniformly infected with *P. infestans*. In contrast, almost 86% of the inoculum is lost from similar-sized plots of corn infected with *P. polysora*.

**Factors affecting level of inoculum gain.** The influence of plot size, spacing between plots, and steepness of the disease gradient on the amount of inoculum exchanged between plots was also predicted by using equation 6. Inoculum exchange decreases with increasing plot spacing; however, as in the case of inoculum loss, disease gradient steepness plays an important role in determining the actual relationship (Fig. 2). Generally, flatter gradients cause a larger proportion of inoculum exchange. For example, inoculum exchange between two 25 $m^2$ square plots spaced 5 m apart will be less than 0.001% of that produced if the disease gradient is fairly steep ($b = 2.0\ m^{-1}$). However, if the gradient is flatter ($b = 0.4\ m^{-1}$), exchange between the same two plots will be over 2.0% of the total inoculum produced. This pattern does not always hold at very small plot spacings because of the relatively uniform (and low) rate of inoculum deposition associated with flat disease gradients.

The quantitative effects of plot spacing and gradient steepness on inoculum exchange were modified slightly by plot size (Fig. 2).

**Determination of gradient steepness (*b*) for potato late blight.** In nonirrigated potato plots, steepness of the primary disease gradient was similar to that in Waggoner's study (15). In our experiments, the value of *b* was calculated as 0.82 $m^{-1}$ in one plot and 1.09 $m^{-1}$ in another. Gradients were steeper in our irrigated plots, with *b* estimated in one case to equal 2.10 $m^{-1}$ (Fig. 3). Data from all plots appeared randomly scattered about fitted regression lines, supporting the validity of equation 2 as a description of the disease

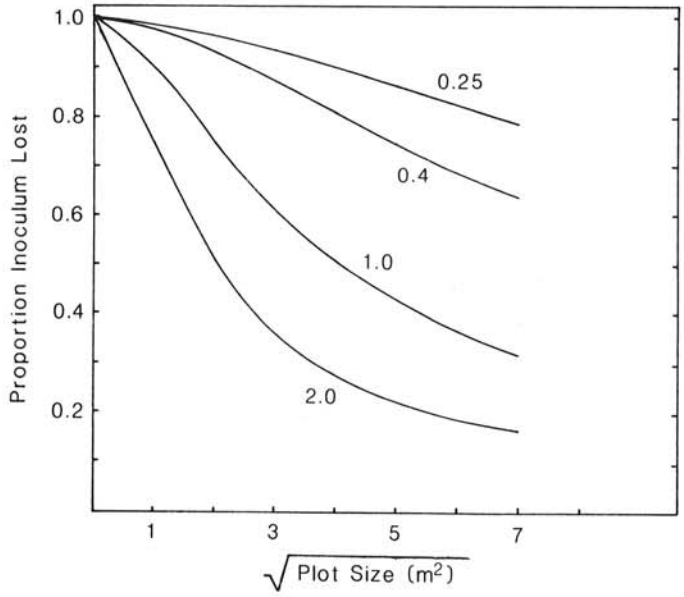


**Fig. 1.** Predicted effect of plot size and gradient steepness on proportion of inoculum of *Phytophthora infestans* lost from square field plots. Number on each line corresponds to the value of *b* ($m^{-1}$) in equation 3.

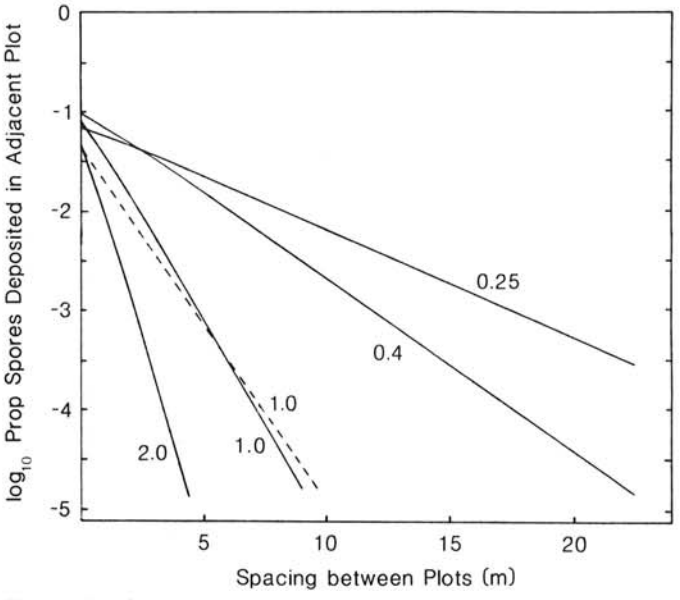


**Fig. 2.** Predicted effects of plot spacing and gradient steepness on proportion of inoculum of *Phytophthora infestans* exchanged between neighboring plots. Number on each line corresponds to the value of *b* ($m^{-1}$) in equation 3. Solid lines represent 25 $m^2$ square plots; the dashed line represents 100 $m^2$ square plots.

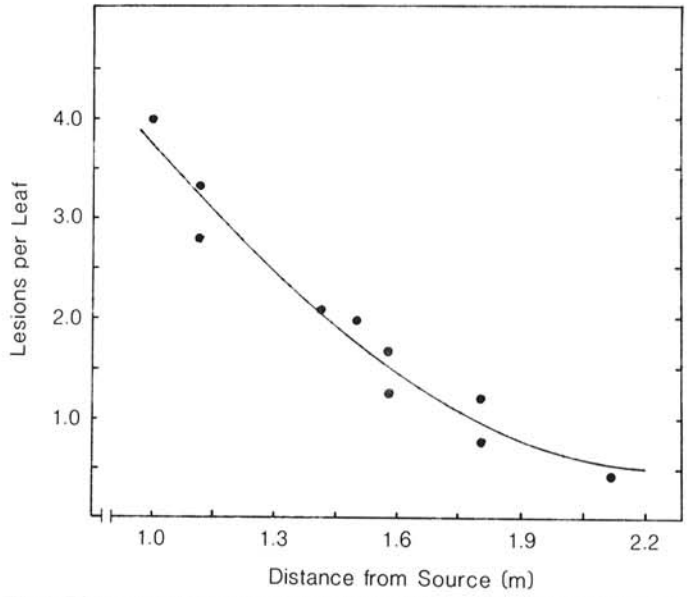


**Fig. 3.** Disease gradient produced by *Phytophthora infestans* in an irrigated potato plot. Lesions were assessed 12 days after inoculation. Each point represents the average of 100–200 leaves. The slope of the line produced by regressing the natural logarithm of lesions per leaf against distance from the source is $-2.1\ m^{-1}$.

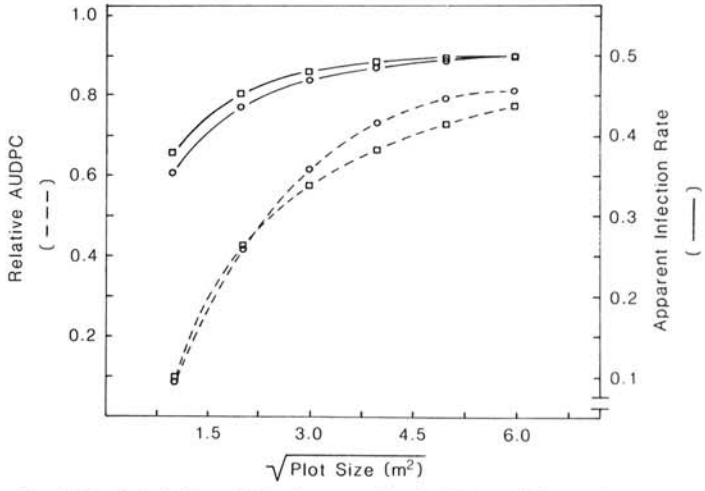


**Fig. 4.** Predicted effect of plot size on epidemic (*Phytophthora infestans* on Kennebec potato) severity using estimated proportions of inoculum loss (assuming $b = 2.0\ m^{-1}$) and two different models of disease development—Bruhn's simulation model (□), and a discrete logistic model (o) as described in the text. Parameter values were selected to produce epidemics in 30 $m^2$ square plots similar to those observed in the largest plots of the 1981 field experiment.

gradient.

**Model validation.** Estimated proportions of inoculum loss were used with two different submodels of disease development in time to predict a relationship between plot size and epidemic severity. Model validation was initiated by comparing predictions with experimental results. Regardless of the model used, predictions were similar (Fig. 4). Both apparent infection rate and AUDPC increased asymptotically with increasing plot size. For $b = 2.0\ m^{-1}$ (similar to that calculated for late blight in irrigated potatoes), the predicted asymptotic limit was approached with plots of about 25–50 $m^2$.

Actual potato late blight development in irrigated field plots of various sizes was qualitatively similar to that predicted by the models (Fig. 5). Since results in 1980 and 1981 were similar, only data from the latter year's experiment are presented. Epidemic severity increased with increasing plot size until plot sizes reached 13–30 $m^2$. The curves shown in Fig. 5 are fitted regression lines with linear and quadratic terms. For both lines, the linear term was highly significant ($P < 0.0001$) while the quadratic term was questionably significant ($P = 0.12$ for AUDPC, $P = 0.04$ for apparent infection rate). The regression lines are not meant to represent the underlying mathematical relationship, they are included only to indicate the qualitative form of the observations.

## DISCUSSION

**Model validation.** The models predicted larger absolute differences in epidemic severity between large and small plots than we observed in field studies (Figs. 4 and 5). Also, the asymptote of maximum epidemic severity was approached with a somewhat smaller plot size than predicted. We believe these incongruities were due primarily to inoculum produced from border plants. Soon after initiation of the experiment, numerous expanding late blight lesions were observed in the borders. These infections were caused by a compatible race of the pathogen that had been used in different experiments nearby and resulted in an unexpected source of positive interference. Because the ratio of border plants to experimental plants was highest in the smallest plots, these plots were subjected proportionately to the largest amount of incoming inoculum, producing smaller treatment differences than expected.

**Model weaknesses and possible modifications.** Although we feel the procedures to be described provide reasonable first approximations of appropriate plot sizes and spacings, it seems possible that some model modifications may be necessary to produce highly accurate guidelines. A few refinements that can easily be incorporated are discussed below.

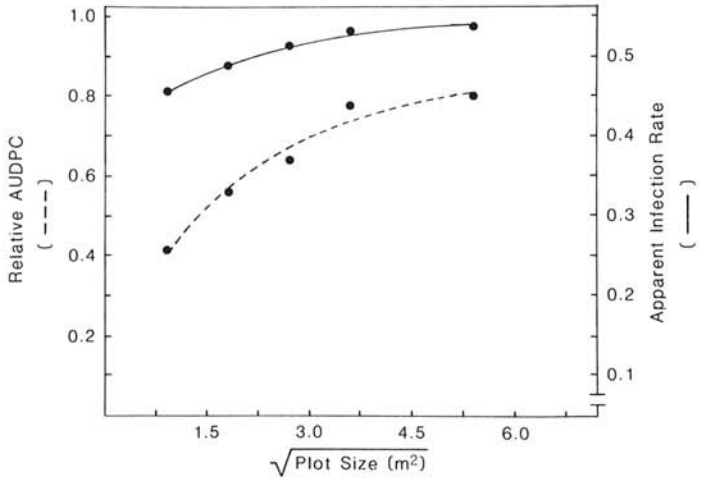


**Fig. 5.** Relationship between plot size and epidemic severity observed in the 1981 field experiment (*Phytophthora infestans* on Kennebec potato). Lines are fitted regressions with linear and quadratic terms. The linear component was highly significant ($P < 0.0001$) for both lines, while the quadratic component was questionably significant ($P = 0.12$ for AUDPC, $P = 0.04$ for apparent infection rate).

The description of disease gradients given by equation 2 is symmetrical, ie, the values of $a$ and $b$ are the same in all directions from the source. Real disease gradients are often asymmetrical owing to special factors (eg, strong prevailing winds). Asymmetry should not cause large errors when calculating proportions of inoculum loss; however, it may cause substantial problems when calculating proportions of inoculum exchanged between plots. Asymmetry can be included in our procedure by dividing the overall gradient into several individual directional sectors, each with its own parameter estimates. The amount of infective inoculum deposited in any target area and the total inoculum produced by the plot (equations 4 and 5) can be found by summing the amounts within each individual sector.

Another assumption of equation 2 is that $b$ remains constant at all distances from the source. In many experiments, individual plots are separated by strips of fallow ground or guard rows consisting of a different plant species or cultivar. This could cause a different rate of inoculum deposition (and hence a different value of $b$) between plots than within them. Lower rates of deposition between plots will result in greater amounts of positive interference than predicted by our model, while higher rates will cause smaller amounts of inoculum exchange. This added complexity could be incorporated by using a second parameter, analogous to $b$, that describes the deposition rate of inoculum between plots. Experimental determination of this rate is feasible, but would be cumbersome.

**Experiment planning.** A model of the disease gradient (equation 3) provides a means of calculating the relative quantities of infective inoculum that are exchanged between plots of an experimental field. The results of these calculations, shown in Figs. 1 and 2, can be used during experiment planning to select plot sizes and spacings that limit interplot interference to some acceptable level. In this paper, we define an acceptable level to be one at which the measure of epidemic behavior (eg, AUDPC) differs by no more than 10% from that which would be found in the absence of interplot interference. This level can be estimated by comparing the behavior of simulated epidemics in the presence and absence of various magnitudes of interplot interference.

The logistic model described by equations 7–9 was used to demonstrate how simulated experimental data can be used to identify acceptable levels of positive interference. We considered a very simple, hypothetical experiment involving two treatments replicated a large number of times. Plots were assumed to be placed in a regular checkerboard arrangement, with every plot neighbored on each of its four sides by a plot that had received the contrasting treatment. Pairs of epidemics corresponding to the two treatments (one relatively fast and one relatively slow), were generated by selecting two different values of the variable $F$ (from equation 9). Several simulations were run using various levels of positive interference (described by $P_i$). It was assumed that a plot received incoming inoculum (positive interference) from only the four nearest neighboring plots, since other plots in a field contribute comparatively little. AUDPC was calculated for both epidemics, and the difference in epidemic severity between treatments was measured as AUDPC of the fast epidemic divided by AUDPC of the slow epidemic ($AUDPC_f / AUDPC_s$). $AUDPC_f / AUDPC_s$ was greatest in the absence of positive interference. As positive interference increased, a point was reached at which $AUDPC_f / AUDPC_s$ began to decline sharply. This point corresponds to the boundary between unacceptable and acceptable amounts of positive interference.

The specific value of this boundary is a function of the magnitude of differences in disease severity between plots. If neighboring plots differ widely, even very low proportions of inoculum exchange can significantly alter epidemic dynamics in the less severely infected plots. Alternatively, if neighboring plots have similar levels of disease, a relatively high proportion of inoculum exchange can occur without significantly influencing epidemic dynamics. This point is illustrated in Fig. 6. By selecting appropriate values of $F$, three experiments were simulated in which the maximum difference in disease severity between treatments was 2-, 10-, and 50-fold. For the experiment with the largest difference, a

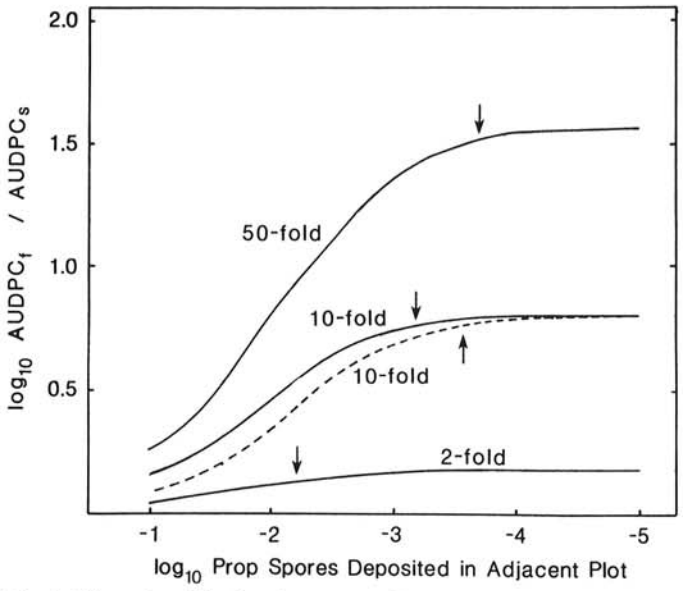


**Fig. 6.** Effect of positive interference on differences between treatments in simulated experiments (based on a model for *Phytophthora infestans* on Kennebec potato). Each line represents a different experiment subjected to various levels of positive interference. Arrows indicate level of positive interference that caused a 10% reduction in observed treatment differences. Curves labeled 2-, 10-, and 50-fold correspond to maximum difference in disease severity between plots when inoculum exchange is zero. Solid lines represent cases in which inoculum loss was 50%, dotted line represents case in which inoculum loss was 75%. The measure of treatment differences is AUDPC of the fast epidemic divided by AUDPC of the slow epidemic (AUDPC$_f$/ AUDPC$_s$). AUDPCs were calculated from day 0 to the time at which disease severity in the fastest epidemic was 0.95.

proportion of inoculum exchange between neighboring plots of only 0.0002 caused a 10% reduction in AUDPC$_f$/ AUDPC$_s$. In contrast, this 10% reduction occurred at a proportion of inoculum exchange of about 0.006 for the experiment with the smallest treatment difference.

Acceptable levels of negative interference can similarly be determined by examining the behavior of epidemics subjected to various amounts of inoculum loss. For example, Fig. 4 can be used directly to select appropriate plot sizes for diseases where $b = 2.0$ m$^{-1}$. In many experiments, particularly those in which disease gradients are relatively flat, plots must be very large to limit inoculum loss to low proportions. In these cases, it may be impractical to eliminate significant levels of negative interference; however, all plots of similar size in an experiment are subject to approximately equal proportions of inoculum loss. If no major interactions occur, substantial levels of negative interference should not have much practical importance.

Negative interference should still be considered, though, because it compounds the effects of positive interference. As a greater proportion of inoculum is lost from a plot, the plot is more easily influenced by incoming external inoculum. For example, in one simulated experiment (Fig. 6), a proportion of inoculum exchange of 0.0006 caused a 10% reduction in AUDPC$_f$/ AUDPC$_s$ when inoculum loss was 50%. However, when inoculum loss was 75%, a 10% reduction occurred with a proportion of inoculum exchange of only 0.0003.

With these simulation results, Figs. 1 and 2 can be used to select appropriate plot sizes and spacings. For example, consider an experiment with two treatments involving a pathogen that produces disease gradients with $b = 1.0$ m$^{-1}$. Assume that it is known from prior experience that the treatments produce epidemics that differ by up to 10-fold in disease severity. Due to practical constraints, the square plots can be no larger than 25 m$^2$. About half of the inoculum is lost from plots of this size (Fig. 1). Fig. 6 indicates an inoculum exchange rate of about 0.0006 can be tolerated without altering epidemic dynamics very much. In this

TABLE 2. Appropriate plot spacings for a hypothetical field experiment[a] that limit positive interference to an acceptable level

| Maximum difference in disease severity[b] | Square plot area (m$^2$) | Estimated plot spacings ($m$) at which positive interference causes a 10% reduction in AUDPC$_f$/ AUDPC$_s$ when the disease gradient ($b$ in units $m^{-1}$) is: | | | |
|---|---|---|---|---|---|
| | | 0.25 | 0.40 | 1.00 | 2.00 |
| 2-fold | 9 | 19.7 | 10.5 | 3.0 | 1.1 |
| | 25 | 16.3 | 9.1 | 2.4 | 0.6 |
| | 100 | 13.5 | 6.7 | 1.4 | 0.2 |
| 10-fold | 9 | 29.4 | 16.1 | 5.3 | 2.3 |
| | 25 | 25.6 | 14.6 | 4.7 | 1.9 |
| | 100 | 22.0 | 12.2 | 4.0 | 1.3 |
| 50-fold | 9 | 35.2 | 19.5 | 6.6 | 2.9 |
| | 25 | 32.0 | 18.2 | 6.0 | 2.6 |
| | 100 | 27.7 | 15.5 | 5.5 | 2.0 |

[a] Experimental layout is described in text.
[b] Differences in disease severity between plots were caused by altering the value of $F$ (infection efficiency) for the two "treatments." Other parameter values were equal for both treatments and arbitrarily selected to create epidemics similar to those of potato late blight in New York. Sensitivity analysis indicated the estimated plot spacings were not substantially affected by the actual parameter values chosen. However, appropriate plot spacings were somewhat wider when epidemic differences were caused by altering $S_\Sigma$ rather than $F$.

experiment, plots should be spaced about 5 m apart (Fig. 2) to limit positive interference to an acceptable level. Several examples of this type are summarized in Table 2.

The method outlined in this paper provides a simple format with which to predict levels of interplot interference in field research. We do not feel the models employed here contain the sophistication required to actually "correct" data gathered from experiments affected by interplot interference; however, the models should be a useful guide in designing future studies. One of the most critical factors in their effective use is the accurate estimation of $b$ for an experimental system. Such gradients will need to be determined experimentally before this method can be applied.

It seems clear that interplot interference can cause treatment differences to be severely underestimated, particularly when dealing with pathogens that produce relatively flat disease gradients, eg, rust and powdery mildew fungi. The current thrust in plant disease management towards efficient and economical means of control demands that quantitative research data accurately reflect phenomena encountered in large-scale commercial agriculture. Reliable data can only be obtained if interplot interference is limited to low levels.

## LITERATURE CITED

1. Bruck, R. I., Fry, W. E., and Apple, A. E. 1980. Effect of metalaxyl, an acylalanine fungicide, on developmental stages of *Phytophthora infestans*. Phytopathology 70:597-601.
2. Bruhn, J. A., and Fry, W. E. 1981. Analysis of potato late blight epidemiology by simulation modeling. Phytopathology 71:612-616.
3. Cammack, R. H. 1958. Factors affecting infection gradients from a point source of *Puccinia polysora* in a plot of *Zea mays*. Ann. Appl. Biol. 46:186-197.
4. Fry, W. E. 1977. Integrated control of potato late blight: Effects of polygenic resistance and techniques of timing fungicide applications. Phytopathology 67:415-420.
5. Fry, W. E. 1978. Quantification of general resistance of potato cultivars and fungicide effects for integrated control of potato late blight. Phytopathology 68:1650-1655.
6. Gregory, P. H. 1968. Interpreting plant disease dispersal gradients. Annu. Rev. Phytopathol. 6:189-212.
7. James, W. C., Shih, C. S., Callbeck, L. C., and Hodgson, W. A. 1973. Interplot interference in field experiments with late blight of potato (*P. infestans*). Phytopathology 63:1269-1275.
8. James, W. C., Shih, C. S., Hodgson, W. A., and Callbeck, L. C. 1976.

Representational errors due to interplot interference in field experiments with late blight of potato. Phytopathology 66:695-700.
9. Jenkyn, J. F., Bainbridge, A., Dyke, G. V., and Todd, A. D. 1979. An investigation into inter-plot interactions, in experiments with mildew on barley, using balanced designs. Ann. Appl. Biol. 92:11-28.
10. Kiyosawa, S., and Shiyomi, M. 1972. A theoretical evaluation of the effect of mixing resistant variety with susceptible variety for controlling plant diseases. Ann. Phytopathol. Soc. Jpn. 38:41-51.
11. Lambert, D. H., Villareal, R. L., and MacKenzie, D. R. 1980. A general model for gradient analysis. Phytopathol. Z. 98:150-154.
12. Paysour, R. E., and Fry, W. E. 1983. Appropriate plot sizes and spacings for field experiments with potato late blight. Pages 150-151 in: Research for the Potato in the Year 2000. W. J. Hooker, ed. International Potato Center, Lima, Peru.
13. Pielou, E. C. 1977. Mathematical Ecology. John Wiley & Sons, New York. 385 pp.
14. Vanderplank, J. E. 1963. Plant Diseases: Epidemics and Control. Academic Press, New York. 349 pp.
15. Waggoner, P. E. 1952. Distribution of potato late blight around inoculum sources. Phytopathology 42:323-328.